Available online at www.sciencedirect.com
ScienceDirect
Ultramicroscopy 107 (2007) 948–953
ultramicroscopy
www.elsevier.com/locate/ultramic

Adhesive interaction measured between AFM probe and lung epithelial type II cells

Zoya Leonenko[a,*], Eric Finot[b], Matthias Amrein[a]

[a]*Department of Cell Biology and Anatomy, Faculty of Medicine, University of Calgary, Alberta, Canada*
[b]*Laboratory of Physics and Nanosciences, Department of Physics, University of Burgundy, Dijon, France*

Received 20 October 2006; accepted 12 February 2007

Abstract

The toxicity of inhaled nanoparticles entering the body through the lung is thought to be initially defined by the electrostatic and adhesive interaction of the particles with lung's wall. Here, we investigated the first step of the interaction of nanoparticles with lung epithelial cells using atomic force microscope (AFM) as a force apparatus. Nanoparticles were modeled by the apex of the AFM tip and the forces of interaction between the tip and the cell analyzed over time. The adhesive force and work of adhesion strongly increased for the first 100 s of contact and then leveled out. During this time, the tip was penetrating deeply into the cell. It first crossed a stiff region of the cell and then entered a much more compliant cell region. The work of adhesion and its progression over time were not dependent on the load with which the tip was brought into contact with the cell. We conclude that the initial thermodynamic aspects and the time course of the uptake of nanoparticles by lung epithelial cells can be studied using our experimental approach. It is discussed how the potential health threat posed by nanoparticles of different size and surface characteristics can be evaluated using the method presented.

Keywords: Atomic force microscopy; Adhesion; Epithelial type II cells

1. Introduction

Elevated levels of ultrafine particles in air pollution are associated with increased morbidity and mortality [1–11]. The critical first step for their toxicity is the penetration of the lung. Unlike larger particles, ultrafine particles reach the peripheral lung and are able to cross the various barriers of the lung, including the lipid–protein layer of pulmonary surfactant at the air–alveolar interface and the cell membranes of the epithelial and endothelial cells underneath and reach the blood stream [9,12–15]. Because of their substantial uptake, ultrafine particles are also of great interest for delivery of drugs to the peripheral lung and the body. Despite the importance of the early penetration steps in the biological effects of inhaled particles, the nature of the interactions with the various barriers of the lung remains poorly understood. A detailed study, therefore, promises substantial progress in the understanding of the health threat posed by fine and ultrafine air pollutants and the effectiveness of drug delivery by aerosols.

In the current study, we measured the adhesion forces between an atomic force microscope (AFM) tip and lung epithelial cells in culture. Most of the lung's interface (>90%) is covered by the very large, thin type I pneumocytes. Gas exchange occurs across these cells and they are the primary target for the airborne nanoparticles. We used primary cell cultures of lung epithelial type II cells (type II pneumocytes) because type I cells do not replicate. Type II cells, after harvesting and growing in media on a glass substrate for a few days, assume a type I phenotype. This change of phenotype is also observed in the lung where type II pneumocyte can replicate to replace damaged type I pneumocytes.

AFM was successfully used before to investigate dynamic and elastic properties of cells [16], cell–cell interaction [17], and adhesion of cells to the various surfaces [18,19]. For most of these studies, a microsphere was attached to a cantilever [20]. Here, we took advantage

*Corresponding author. Tel.: +1 403 210 3809.
E-mail address: zleonenk@ucalgary.ca (Z. Leonenko).

0304-3991/$ - see front matter © 2007 Elsevier B.V. All rights reserved.
doi:10.1016/j.ultramic.2007.02.036

of the small radius of curvature of unaltered AFM tips to mimic the interaction between nanoparticles and the lung epithelial cells.

2. Materials and methods

2.1. Cell culture

Lung epithelial cells, type II, were isolated from male, pathogen free, Sprague–Dawley rats weighing 150–250 g. The cells were cultured at 6×10^8 cells/mL in DMEM medium supplemented with 1% L-glutamine, containing 10% heat-inactivated FBS, 300 μL of the solution Penicillin/Gentamycin in γ-irradiated culture dishes. The cells were grown on light microscope glass coverslips. The cells were kept in an incubator under 5% CO_2 and 37 °C until they created a monolayer with approximately 80% of confluence (4–6 days). At this stage, the phenotype of the lung epithelial cells had changed from type II to type I in that the cells were spread out flat on the interface and ceased to produce surfactant.

2.2. Force spectroscopy

Lung epithelial cells were first imaged in a light microscope (Zeiss Axiovert 200). For the force spectroscopy, a NanoWizard-AFM (JPK, Instruments AG, Berlin) was used. The AFM tip was used as a model for a nanoparticle, approaching the cell. The AFM tip was positioned above the cell nucleus under optical control. Cantilevers (Micromash) with the spring constant 57 mN/m and pyramidal silicon nitride tips were used (tip height: 2.9 μm, tip radius: less than 20 nm (typical 10 nm), tip angle (face to face): 25–45° (top to around 300 nm down). Forces of interaction between the probe and the cell were then measured in medium at 35 °C, by approaching the tip to the cell interface until a preset load was reached (trace of force curve). The force was acquired as a function of the tip–sample separation h. After the tip has come into contact with the cell, h becomes the penetration depth for the tip into the cell. Separate force curves were acquired for a preset load of 100, 200, and 300 pN. The tip was now kept in contact with the cell for a pre-determined time, while keeping the preset load constant under feedback control (i.e., when the load decreased, the tip was moved forward). Then, the tip was retracted from the cell (retrace of the force curve). Cells were kept in medium at all times.

2.3. Analysis

The spring constant for each cantilever was measured before and after the experiment using the procedures implemented by the manufacturer of the AFM (thermal noise method). Sensitivity and spring constant were found to be not different before and after the experiment.

The approach part of the force curve was used to determine the depth to which the tip penetrated the cell as well as the mechanical properties of the sample. The penetration depth was measured from the point where the tip came into contact with the cell (denoted by 2 in Fig. 1). This point is apparent in the force curve as the first upward deflection of the force curve when following the trace of the force curve.

To evaluate the mechanical properties of the sample from the approach force profile, the Sneddon model was employed [21,22]. As the penetration depth h of the tip into the cell can be around 1 μm, the geometry of the tip must be considered as a function of the penetration depth. The effective Young's modulus, E', was estimated point by point for h as follows: considering the geometry of the tip, the three regions have to be justified [23]:

For h between 0 and 10 nm, the AFM probe was considered as a hemi-sphere with a radius R of 10 nm

$$E_{\text{sphere}} = \frac{3}{4\sqrt{R}} \frac{F}{h^{3/2}}.$$

For further penetration, the tip profile was viewed as a cone whose half angle α vary linearly from $\alpha_1 = 25^\circ$ at $h = 10$ nm up to $\alpha_2 = 45^\circ$ when h reaches 300 nm.

$$E_{\text{cone}} = \frac{\sqrt{2}}{\tan \alpha} \frac{F}{h^2}$$

For an indentation deeper than 300 nm, the cone angle is considered constant to α_2.

The retrace curve was used to calculate the adhesion energy Γ between tip and cell:

$$\Gamma = \sum_{h_1}^{h_2} F_{\text{retrace}}(h_i)(h_{i+1} - h_i).$$

F_{retrace} (h_i) is the adhesion force at h_1. h_1 is the point of the initial contact between the tip and the cell surface (denoted by 2 in Fig. 1). h_1 was determined from the approach part of the force curve. h_2 corresponds to the last jump out of contact.

3. Results and discussions

Type I lung epithelial cells cover about 95% of the lung's interface to the air and are therefore the primary target of airborne nanoparticles entering the lung. Fig. 1A shows the lung epithelial cells used in the current study. The cells were grown on a glass coverslip in a primary culture from type II lung epithelial cells from rats. The cells had assumed a type I phenotype after about 2 days in culture. They had changed from a more cubical shape into flat cells and became increasingly confluent. Type I cells cannot directly be grown in a primary culture because they do not replicate.

For force spectroscopy, a media-covered coverslip with the cells was mounted in the liquid cell of the AFM. The setup used allows for the observation of the sample across the coverslip from below by an inverted light microscope at the same time as force spectroscopy (or AFM imaging) is

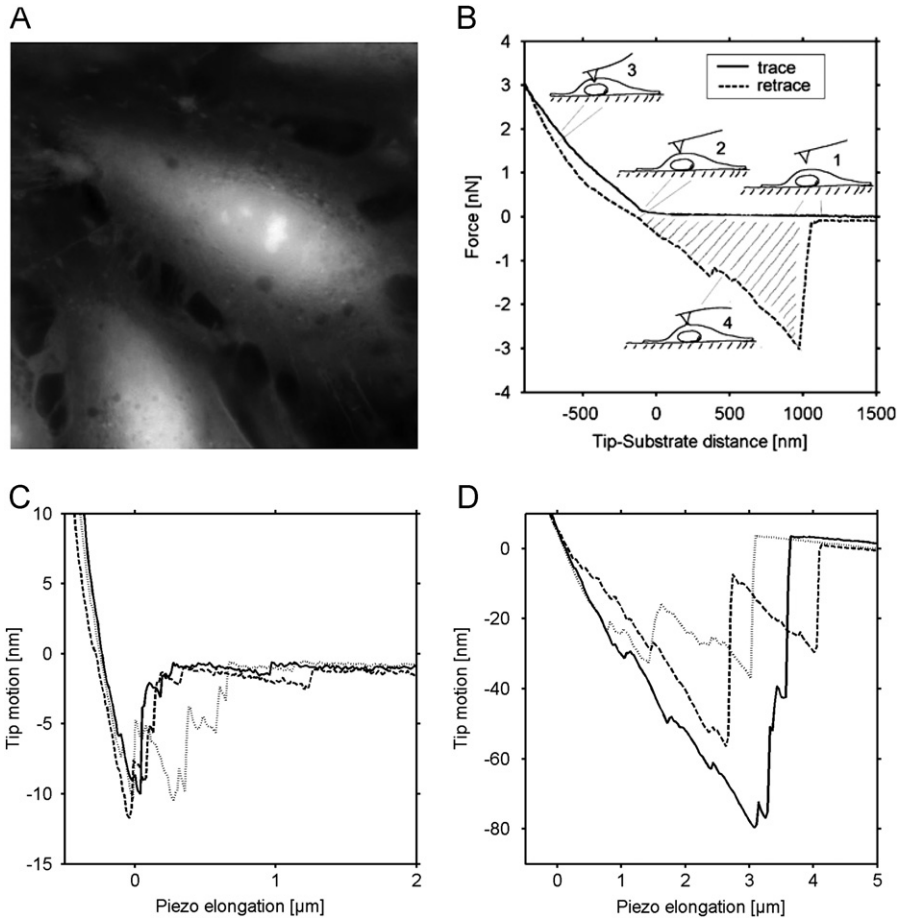

Fig. 1. A. Dark-field light micrograph of two lung epithelial cells (75 μm × 75 μm). For force spectroscopy, an AFM tip was placed over the central region of a cell. Trace and retrace force curves were measured on a cell. Force versus tip–sample separation is shown on (B). The approach part (trace) reveals how the cell deforms upon the impact of the tip. The retrace or withdraw part of the curve reveals a large adhesion peak, which is often split in multiple peaks. The sketches explain the physical situation for each part of the curve. The hatched area denotes the work of adhesion (adhesion energy) between tip and cell. The AFM tip was allowed to stay in contact for various times (delay time). Typical raw data (cantilever deflection versus piezo displacement) are shown on Fig. 1C and D, which correspond to delay time 30 s (C) and 300 s (D) accordingly.

performed. The tip of the AFM was thus placed over a suitable cell and cell location under light microscope control. Fig. 1B shows a typical force scan. At first, the probe approached the cell with the lever undeflected (horizontal line of the force trace), indicating no interaction. The tip then made contact with the sample and became deformed. The tip was then kept in contact with the cell for various times. We varied the delay time from 0 to 1800 s. Fig. 1C and D show typical raw data force plots collected at delay times 30 and 300 s. Thereafter, the tip was retracted and the adhesion observed. Unlike the experiment shown in Fig. 1B, for all experiments the maximum load for the tips onto the cells was kept at 100, 200, or 300 pN. In the following sections we will discuss the fast initial penetration of the cells followed by an analysis of the interaction over time.

Upon the approach, the tips instantly penetrated the cells by approximately 500 nm, irrespective of the load chosen. The trace part of the force curve was used to analyze the Young's modulus of the cells using Sneddon's model as the tip was penetrating deeper into the interior (Fig. 2). At first, the tip experienced a layer of increasing stiffness to a penetration depth of about 100 nm at which point the resistance of the cell to penetration reached a maximum. Thereafter the cell became more compliant again. The stiff layer may represent the outer layer of the cytoskeleton anchored to the cell membrane.

The analysis of the forced indentation of the epithelial cells by the tip as shown in Figs. 1 and 2 reveals the fate of a nanoparticle coming into contact with the lung's epithelium and then being actively loaded onto a cell. This situation will indeed occur in the lung. The lung's epithelium toward the air is covered by a thin aqueous layer and a molecular film of pulmonary surfactant at the air–water interface. Transmission electron microscopy of lung's thin sections as well as scanning electron microscopy of the lung has indeed shown that particles trapped between the surfactant layer and the epithelial cells strongly deform the cells [24,25].

After the initial indentation, the tip was kept loaded onto the cell with 200 pN for preset times ranging from 0 to 900 s under feedback control (i.e., when the load decreased over

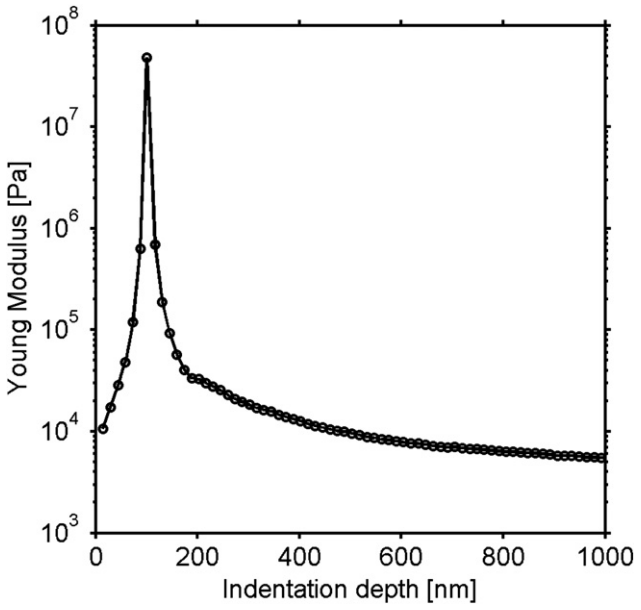

Fig. 2. When analyzing the approach curve, one can determine the Young's modulus of the sample surface. Young's modulus, which gives a measure of cell elasticity in our case, was found to depend on indentation depth, showing two distinctive parts of the plot: when penetrating the peripheral part of the cell, up to about 100 nm into the cell, the cell became increasingly stiffer. The stiffness then dropped sharply upon further penetration until it leveled out after penetrating about 200 nm deep.

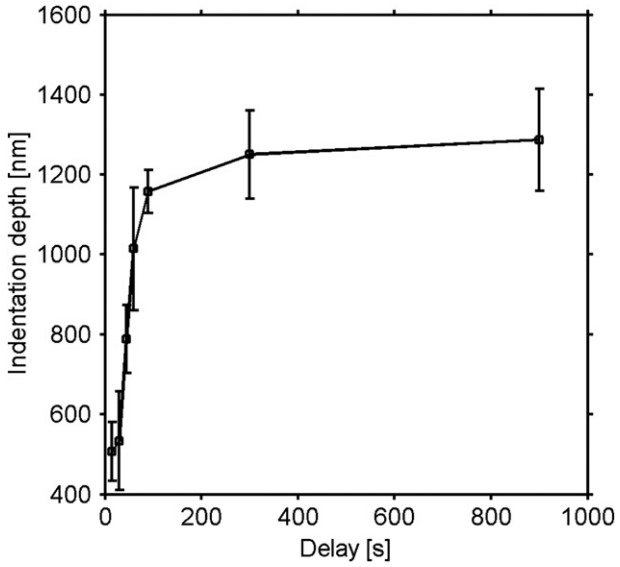

Fig. 3. Indentation depth as a function of time. The load was kept constant at 200 pN. At time 0, the indentation was about 500 nm. Over time, the tip first penetrated rapidly and then slowly from 500 to 1300 nm. This is evidence a time-dependent response of the cell to the tip.

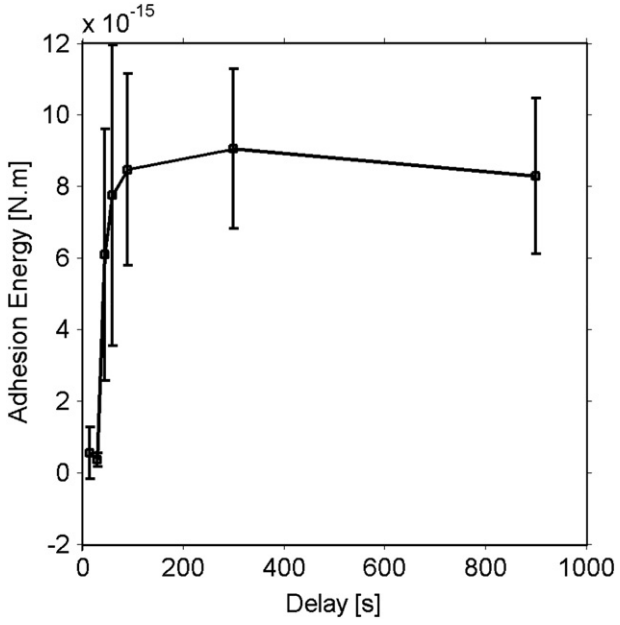

Fig. 4. Adhesive energy as a function of the time, the tip was kept in contact with the cell at a constant load of 200 pN. The adhesive energy is revealed upon retraction of the tip as explained in Fig. 1. The longer the tip stays in contact with the cell the larger adhesion is observed. Statistical analysis shows that considerable changes occur during first 100 s after which the adhesion energy no longer changes.

time, the tip was moved forward Fig. 3). During the first 100 s, the tip rapidly penetrated the cell from 500 to about 1000 nm and then slowly came to a halt. Interestingly, a similar behavior was also observed when the load was either kept constant at 100 or at 300 pN (not shown). This as well as the time course of the penetration is indicative that the process observed cannot be explained as the passive penetration of a viscous medium. Rather we assume that the tip is either actively uptaken or the cell rearranges its plasma membrane and the cytoskeleton elements to accommodate the tip.

With the increase of the delay time, the adhesive energy also increases (Fig. 4). This process comes to an end after about 100 s. Both adhesion energy and the penetration of the tip into the cell increase with the larger contact time. The increase in the adhesion energy correlates with the increase of indentation depth (Fig. 5). This indicates that the tip becomes engulfed by the membrane and the area of interaction increases (Fig. 4). In conclusion, if the tip were an isolated nanoparticle, it would be uptaken after this time.

Our results suggest a process of particle uptake by lung epithelial cells that occurs over approximately 100 s during which time the tip (nanoparticle) increases its adhesive interaction and penetrates the cell. Particles of this size are not phagocytosed [12,26]. They enter cells in the absence of clathrin and caveolin, associated with active uptake and even when an actin-based mechanism has been ruled out [26] have also shown that nanoparticles inside a cell are not surrounded by membrane and, hence, are not uptaken through vesicle formation [12,26].

Our findings suggest that irrespective of the exact mechanism, particle submersion in the epithelial cells seem to depend on the adhesive interaction. The adhesive interaction includes electrostatic, van der Waals, steric

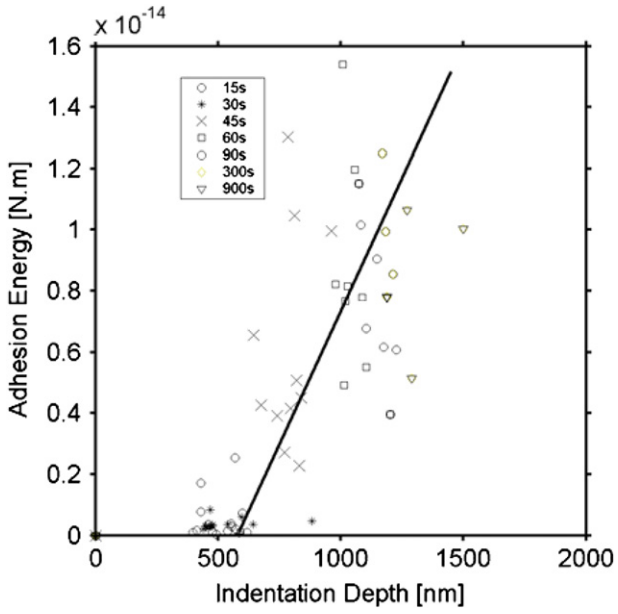

Fig. 5. Adhesive energy as a function of indentation, plotted for various time points. The increase in adhesion energy correlates with the increase in indentation depth.

and hydrophobic forces as well as the line tension between particle, cell and aqueous medium and depends on the elastic and plastic properties of the cell. The free energy due to these interactions will be minimized upon particle wetting by the lining layer. The lower the surface free energy of the particle, the lesser it will be wetted by the cell. A thermodynamic model using the ''wettability criterion'' was indeed successful in predicting passive particle uptake by cells [27]. Another thermodynamic analysis combined with a molecular dynamics simulation found negative line tension values for nanometer-sized particles, but positive values for those an order of magnitude larger [28]. The engulfment of particles in the nanometer range by unbalanced capillary forces was suggested by Shanahan [29] and more recently by Livadaru and Kovalenko [30].

3.1. Future perspectives

The role of the adhesive interaction in particle uptake can now be put to the test using our approach. Particles of different surface properties and different geometries can be mimicked by according AFM tips. The adhesive interaction of a particle with the plasma membrane in the lung depends also on the particle history. Airborne particles, after crossing a surfactant layer at the air–water interface of a cell culture dish, have been shown to be more readily uptaken than particles added to the media [31]. They may have become coated with a film of pulmonary surfactant and, as a consequence, have penetrated the epithelial cells differently. Whether this is related to a change in adhesive interaction can be tested by coating AFM tips with surfactant.

Acknowledgements:

Financial support from Canadian Institute of Health Research and Department of Physics, University of Burgundy, France, is greatly appreciated, as well as technical support from JPK Instrument, Berlin, Germany and Microscopy and Imaging Facility, University of Calgary. The authors thank Dr. Christian La Grimmellec and Dr. Samuel Schurch for helpful discussions, Spomenka Curic for the preparation of the lung epithelial cells, and Dr. W. Michael Schoel for the light micrograph of Fig. 1.

References

[1] R.W. Atkinson, H.R. Anderson, D.P. Strachan, J.M. Bland, S.A. Bremner, A.P. de Leon, Eur. Respir. J. 13 (1999) 257.
[2] F. Ballester, P. Rodriguez, C. Iniguez, M. Saez, A. Daponte, I. Galan, M. Taracido, F. Arribas, J. Bellido, F.B. Cirarda, A. Canada, J.J. Guillen, F. Guillen-Grima, E. Lopez, S. Perez-Hoyos, A. Lertxundi, S. Toro, J. Epidemiol. Community Health 60 (2006) 328.
[3] R.D. Brook, B. Franklin, W. Cascio, Y.L. Hong, G. Howard, M. Lipsett, R. Luepker, M. Mittleman, J. Samet, S.C. Smith, I. Tager, Circulation 109 (2004) 2655.
[4] F. Dominici, R.D. Peng, M.L. Bell, L. Pham, A. McDermott, S.L. Zeger, J.M. Samet, JAMA 295 (2006) 1127.
[5] R.D. Brook, Current Hypertension Reports 7 (2005) 427.
[6] A.C. Elder, R. Gelein, J.N. Finkelstein, C. Cox, G. Oberdorster, Inhal. Toxicol. 12 (2000) 227.
[7] M.S. Goldberg, R.T. Burnett, J.F.O. Yale, M.F. Valois, J.R. Brook, Environ. Res. 100 (2006) 255.
[8] G. Oberdorster, E. Oberdorster, J. Oberdorster, Environ. Health Perspect. 113 (2005) 823.
[9] G. Oberdorster, Z. Sharp, V. Atudorei, A. Elder, R. Gelein, A. Lunts, W. Kreyling, C. Cox, J. Toxicol. Environ. Health 65 (2002) 1531.
[10] U. Poschl, Angew. Chem. Int. Ed. 44 (2005) 7520.
[11] J. Schwartz, F. Laden, A. Zanobetti, Environ. Health Perspect. 110 (2002) 1025.
[12] M. Geiser, B. Rothen-Rutishauser, N. Kapp, S. Schurch, W. Kreyling, H. Schulz, M. Semmler, V.I. Hof, J. Heyder, P. Gehr, P. Environ. Health Perspect. 113 (2005) 1555.
[13] A. Nemmar, P.H.M. Hoet, B. Vanquickenborne, D. Dinsdale, M. Thomeer, M.F. Hoylaerts, H. Vanbilloen, L. Mortelmans, B. Nemery, Circulation 105 (2002) 411.
[14] A. Nemmar, H. Vanbilloen, M.F. Hoylaerts, P.H.M. Hoet, A. Verbruggen, B. Nemery, Am. J. Respir. Crit. Care Med. 164 (2001) 1665.
[15] S. Takenaka, E. Karg, C. Roth, H. Schulz, A. Ziesenis, U. Heinzmann, P. Schramel, J. Heyder, Environ. Health Perspect. 109 (2001) 547.
[16] F. Rico, P. Roca-Cusachs, N. Gavara, R. Farre, M. Rotger, D. Navajas, Phys. Rev. E 72 (2005) 021914.
[17] A. Ikai, R. Afrin, Cell Biochem. Biophys. 39 (2003) 257.
[18] G. Sagvolden, I. Giaever, E.O. Pettersen, J. Feder, Biophysics 96 (1999) 471.
[19] E.P. Wojcikiewicz, X. Zhang, V.T. Moy, Biol. Proced. Online 6 (2004) 1.
[20] M. Kappl, H.-J. Butt, Part. Part. Syst. Char. 19 (2002) 129.
[21] J.N. Sneddon, Int. J. Eng. Sci. 3 (1965) 47.
[22] B. Cappella, G. Dietler, Surf. Sci. Rep. 34 (1999) 1.
[23] R.W. Stark, T. Drobek, M. Weth, J. Frickef, W.M. Heckel, Ultramicroscopy 75 (1998) 161.
[24] H. Bachofen, S. Schurch, F. Possmayer, J. Appl. Physiol. 76 (1994) 1983.

[25] P. Gehr, M. Geiser, V. Im Hof, S. Schurch, U. Waber, M. Baumann, Microsc. Res. Tech. 26 (1993) 423.
[26] B.M. Rothen-Rutishauser, S. Schurch, B. Haenni, N. Kapp, P. Gehr, Environ. Sci. Technol. 40 (2006) 4353.
[27] H. Chen, R. Langer, D.A. Edwards, J. Colloid Interface Sci. 190 (1997) 118.
[28] F. Bresme, N. Quirke, J. Chem. Phys. 110 (1999) 3536.
[29] M.E.R. Shanahan, J. Phys. D Appl. Phys. 23 (1990) 321.
[30] L. Livadaru, A. Kovalenko, Nano Lett. 6 (2006) 78.
[31] F. Blank, B.M. Rothen-Rutishauser, S. Schurch, P. Gehr, Journal of Aerosol Medicine 19 (2006) in press.